

# SWiFT Wake Steering

## Instrumentation and Data Processing

### Table of Contents

<b>Nomenclature .....</b>	<b>2</b>
<b>1 SWiFT Site Layout and Coordinate System .....</b>	<b>3</b>
<b>2 Data Channels .....</b>	<b>5</b>
2.1 Meteorological Tower Channel Listing.....	6
2.2 Wind Turbine Channel Listing.....	8
2.3 Lidar Channel Listing.....	9
<b>3 National Instruments CompactRIO .....</b>	<b>10</b>
<b>4 Meteorological Towers.....</b>	<b>10</b>
4.1 Sonic Anemometers.....	10
4.2 Cup Anemometers.....	10
4.3 Wind Vane .....	11
4.4 Barometric Pressure .....	11
4.5 Relative Humidity .....	11
4.6 Temperature .....	11
<b>5 Turbine Sensors.....</b>	<b>11</b>
5.1 Nacelle Wind Sensor .....	11
5.2 Yaw Heading .....	12
5.3 Azimuth Angle .....	12
5.4 Low Speed Shaft Tachometer .....	12
5.5 High Speed Shaft Tachometer – Smoothed .....	12
5.6 Generator Power and Generator Torque .....	12
5.7 Blade Pitch .....	12
<b>6 Lidar Data .....</b>	<b>13</b>
<b>7 References .....</b>	<b>17</b>

DOCUMENT REVISION LOG			
<b>Document Title:</b> Scaled Wind Farm Technology (SWiFT) Facility Wake Steering Experiment Instrumentation and Data Processing SAND2017-3252 O			
<b>Document Owner(s):</b> Brian Naughton, Experiment PI			
Revision	Date	Author(s)/Approval	Summary of Change(s)
0	3-20-2017	Brian Naughton	

## Nomenclature

A2e	Atmosphere to electrons
DAP	Data Archive and Portal
DTU	Technical University of Denmark
GPS	Global Positioning System
MET	meteorological tower
NaN	Not a Number
SWiFT	Scaled Wind Farm Technology
TAI	International Atomic Time
TST	total station theodolite
UTC	Coordinated Universal Time
WTG	wind turbine generator

# 1 SWiFT Site Layout and Coordinate System

The Sandia National Laboratories operates the Scaled Wind Farm Technology (SWiFT) facility located at Texas Tech University's National Wind Institute Research Center in Lubbock, Texas. The baseline instrumentation includes three research wind turbines and two meteorological towers as shown in Figure 1. The approximate locations of these assets are noted in Table 1.

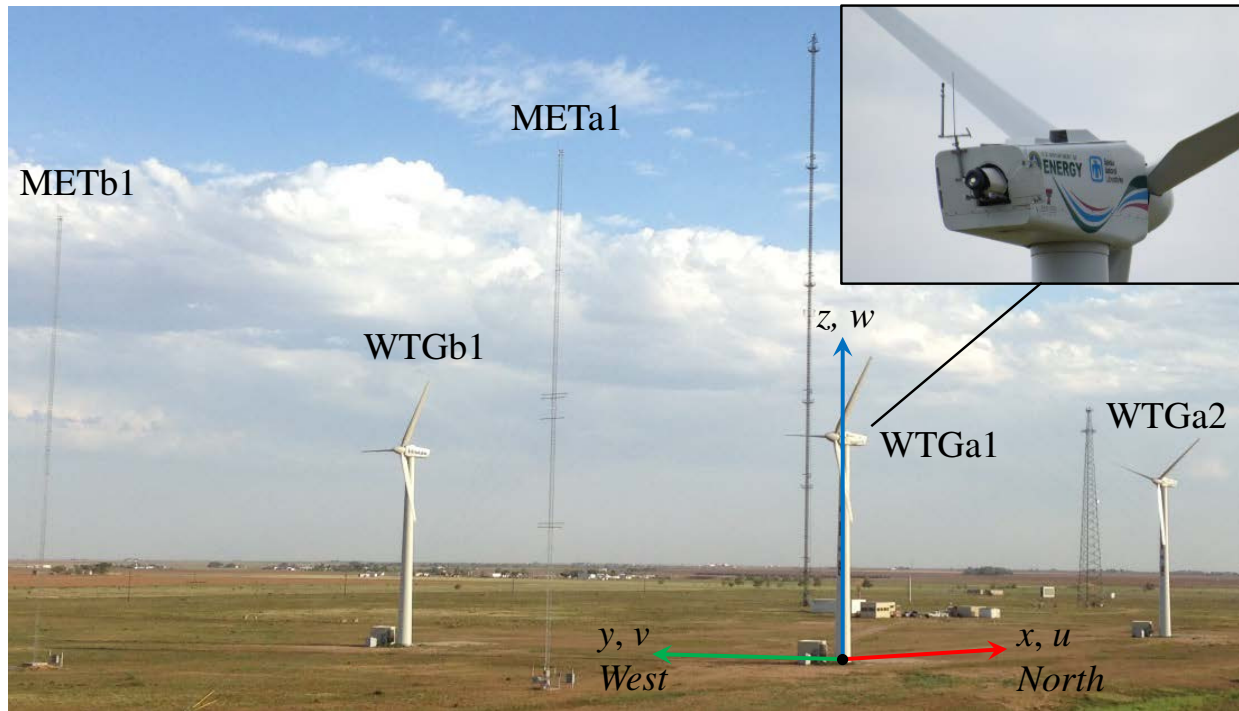


Figure 1. SWiFT facility layout and coordinate system with the DTU SpinnerLidar installed in WTGa1 [1].

Table 1. Locations of the primary instrument assets at the SWiFT facility (GPS coordinates of WTGa1 are approximately: Lat. 33.60795°, Lon. -102.04862°, Base Elevation 1018.0 m).

Instrument	$x$ (m), North	$y$ (m), West	$z$ (m), Base Height
WTGa1	0.00	0.00	0.00
WTGa2	134.97	0.17	0.09
WTGb1	-5.41	80.95	-0.02
METa1	-69.50	-3.29	0.22
METb1	-74.95	77.53	0.20

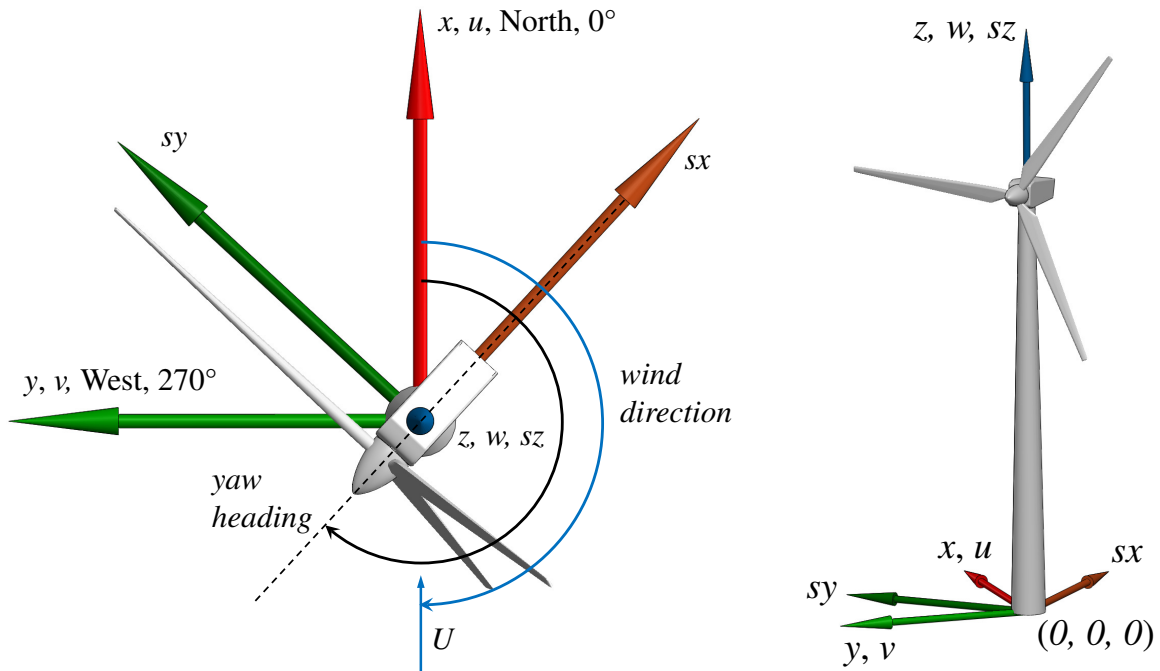


Figure 2. Schematic of the SWiFT site coordinate system relative to the lidar coordinate system ( $sx, sy, sz$ ).

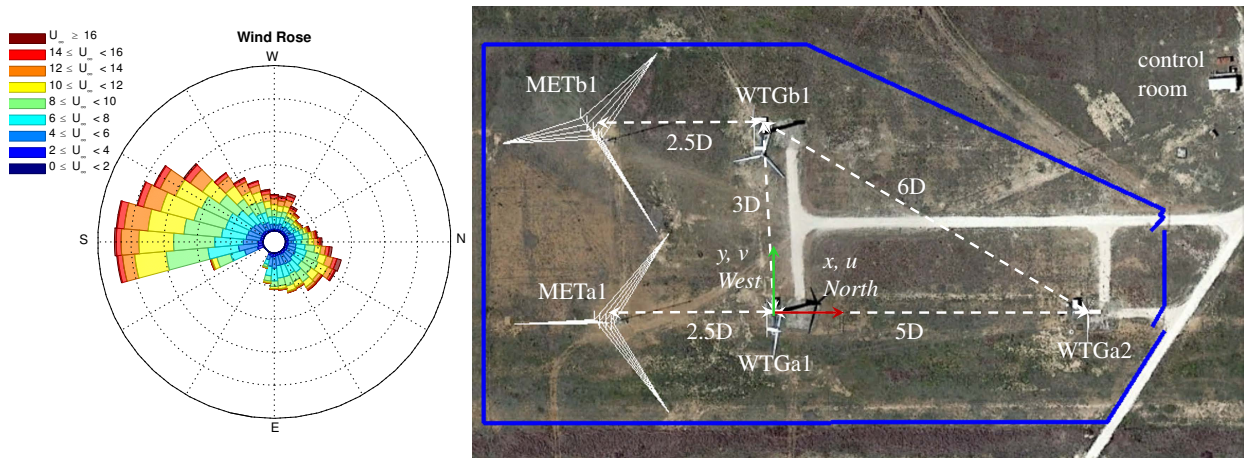


Figure 3. Top view of the SWiFT facility layout and wind rose ( $D = 27\text{m}$ ) [2].

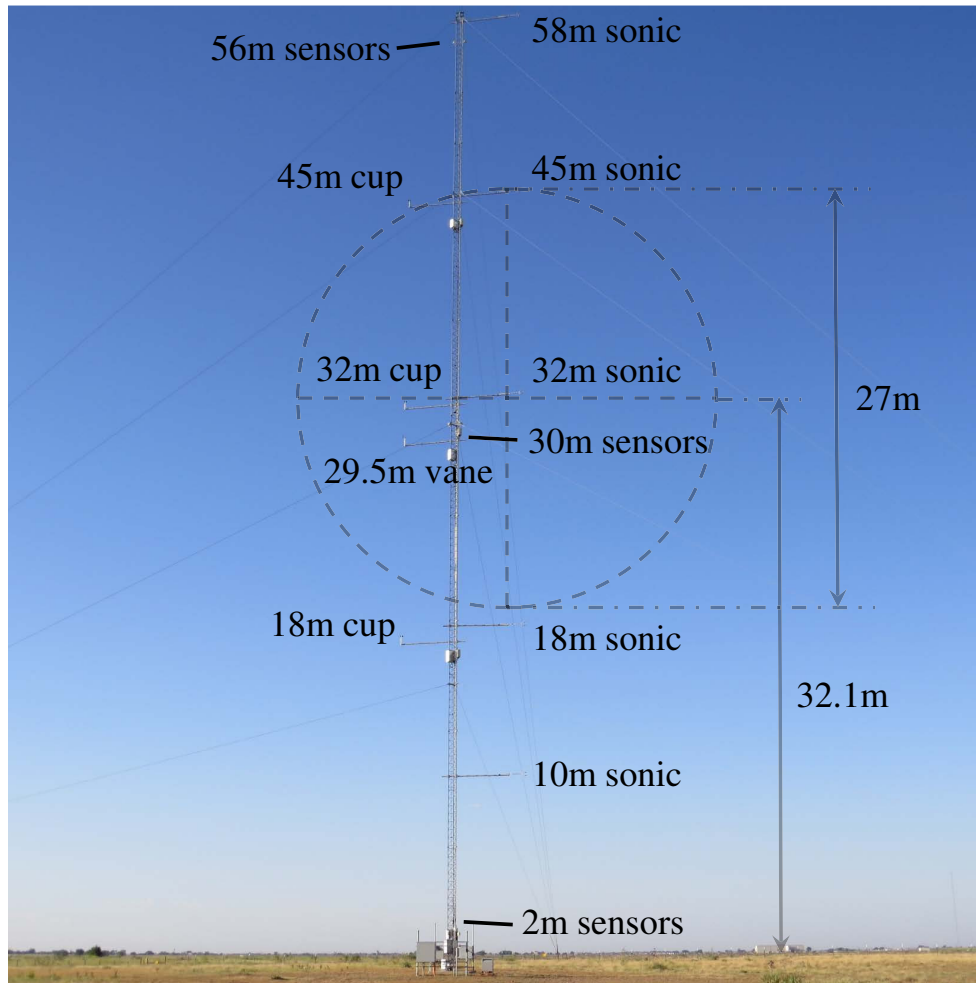


Figure 4. Photo of the METa1 sonic anemometers and atmospheric sensors (temperature, relative humidity, barometric pressure). The image was acquired looking in the Southerly direction and includes an approximate projection of the WTGa1 rotor diameter on the met tower.

## 2 Data Channels

The logged SWiFT facility data are grouped into three approximately 10 minute files corresponding to the met sensors, wind turbine sensors, and lidar measurements. The files follow the DOE Atmosphere to electrons Data Archive and Portal (A2e DAP) naming convention of:

`met.z01.b0.start_date(yyyymmdd).start_time(HHMMSS)` for the met tower data channels

`turbine.z01.b0.start_date(yyyymmdd).start_time(HHMMSS)` for the wind turbine data channels

`lidar.z01.b0.start_date(yyyymmdd).start_time(HHMMSS)` for the lidar data channels

The time stamps on the SWiFT data are provided as datenum units. Datenum is a time unit represented as the number of days from the epoch January 0, 0000. The data is provided in the

International Atomic Time (TAI) time standard. The SWiFT site natively acquires data using GPS synced TAI time stamps which include leap seconds. The TAI time standard is similar to Coordinated Universal Time (UTC), where currently, TAI is exactly 37 seconds ahead of UTC, including the initial 10 second difference plus the accumulation of 27 leap seconds since 1972.

The data channels indicating directionality within the  $x$ - $y$  plane have units of degN, indicating the number of degrees clockwise from North as shown in Figure 2. North is represented as 0 degN.

## 2.1 Meteorological Tower Channel Listing

Channel	Description	Units
atmoSensors_data(1)	Time	datetime
atmoSensors_data(2)	BP02m	mbar
atmoSensors_data(3)	BP30m	mbar
atmoSensors_data(4)	RH02m	pct
atmoSensors_data(5)	RH30m	pct
atmoSensors_data(6)	RH56m	pct
atmoSensors_data(7)	Temp02m	degC
atmoSensors_data(8)	Temp30m	degC
atmoSensors_data(9)	Temp56m	degC
atmoSensors_data(10)	WindDirectionVane29m	degN
atmoSensors_data(11)	WindSpeedCup18m	m/s
atmoSensors_data(12)	WindSpeedCup32m	m/s
atmoSensors_data(13)	WindSpeedCup45m	m/s
sonic10m_data(1)	Sonic10_time	datetime
sonic10m_data(2)	Sonic10_u	m/s
sonic10m_data(3)	Sonic10_v	m/s
sonic10m_data(4)	Sonic10_w	m/s
sonic10m_data(5)	Sonic10_ws	m/s
sonic10m_data(6)	Sonic10_wd	degN
sonic10m_data(7)	Sonic10_temp	degC
sonic18m_data(1)	Sonic18_time	datetime
sonic18m_data(2)	Sonic18_u	m/s
sonic18m_data(3)	Sonic18_v	m/s
sonic18m_data(4)	Sonic18_w	m/s
sonic18m_data(5)	Sonic18_ws	m/s
sonic18m_data(6)	Sonic18_wd	degN
sonic18m_data(7)	Sonic18_temp	degC
sonic32m_data(1)	Sonic32_time	datetime
sonic32m_data(2)	Sonic32_u	m/s
sonic32m_data(3)	Sonic32_v	m/s
sonic32m_data(4)	Sonic32_w	m/s
sonic32m_data(5)	Sonic32_ws	m/s

sonic32m_data(6)	Sonic32_wd	degN
sonic32m_data(7)	Sonic32_temp	degC
sonic45m_data(1)	Sonic45_time	datetime
sonic45m_data(2)	Sonic45_u	m/s
sonic45m_data(3)	Sonic45_v	m/s
sonic45m_data(4)	Sonic45_w	m/s
sonic45m_data(5)	Sonic45_ws	m/s
sonic45m_data(6)	Sonic45_wd	degN
sonic45m_data(7)	Sonic45_temp	degC
sonic58m_data(1)	Sonic58_time	datetime
sonic58m_data(2)	Sonic58_u	m/s
sonic58m_data(3)	Sonic58_v	m/s
sonic58m_data(4)	Sonic58_w	m/s
sonic58m_data(5)	Sonic58_ws	m/s
sonic58m_data(6)	Sonic58_wd	degN
sonic58m_data(7)	Sonic58_temp	degC
sonic_pos_data(1)	Sonic10_position	x(m), y(m), z(m)
sonic_pos_data(2)	Sonic18_position	x(m), y(m), z(m)
sonic_pos_data(3)	Sonic32_position	x(m), y(m), z(m)
sonic_pos_data(4)	Sonic45_position	x(m), y(m), z(m)
sonic_pos_data(5)	Sonic58_position	x(m), y(m), z(m)
atmoSensors_pos_data(1)	WindDirectionVane29m_position	x(m), y(m), z(m)
atmoSensors_pos_data(2)	WindSpeedCup18m_position	x(m), y(m), z(m)
atmoSensors_pos_data(3)	WindSpeedCup32m_position	x(m), y(m), z(m)
atmoSensors_pos_data(4)	WindSpeedCup45m_position	x(m), y(m), z(m)
atmoSensors_pos_data(5)	BP_RH_Temp_02m_position	x(m), y(m), z(m)
atmoSensors_pos_data(6)	BP_RH_Temp_30m_position	x(m), y(m), z(m)
atmoSensors_pos_data(7)	RH_Temp_56m_position	x(m), y(m), z(m)
atmoSensors_variables	variable list corresponding to atmoSensors_data	
stmoSensors_units	unit list corresponding to atmoSensors_data	
sonic_10m_variables	variable list corresponding to sonic_10m_data	
sonic_10m_units	unit list corresponding to sonic_10m_data	
sonic_18m_variables	variable list corresponding to sonic_18m_data	
sonic_18m_units	unit list corresponding to sonic_18m_data	
sonic_32m_variables	variable list corresponding to sonic_32m_data	
sonic_32m_units	unit list corresponding to sonic_32m_data	
sonic_45m_variables	variable list corresponding to sonic_45m_data	
sonic_45m_units	unit list corresponding to sonic_45m_data	
sonic_58m_variables	variable list corresponding to sonic_58m_data	
sonic_58m_units	unit list corresponding to sonic_58m_data	
sonic_pos_variables	variable list corresponding to sonic_pos_data	

sonic_pos_units	unit list corresponding to sonic_pos_data
atmoSensors_pos_variables	variable list corresponding to atmoSensors_pos_data
atmoSensors_pos_units	unit list corresponding to atmoSensors_pos_data

## 2.2 Wind Turbine Channel Listing

Channel	Description	Units
data(1)	Time	datenum
data(2)	NacWindSpeed	m/s
data(3)	NacWindDir	deg
data(4)	YawHeading	deg
data(5)	Azimuth	deg
data(6)	LSSTach1	rpm
data(7)	HSSTach1_Smooth	rpm
data(8)	GenPwr	kW
data(9)	GenTq	Nm
data(10)	BldPitch1	deg
variables	list of variables	
units	list of variable units	



## 2.3 Lidar Channel Listing

Channel	Description	Units
scan_index	index of scan point for each scan (nested cells)	
scan_datenum	datenum of every scan position (nested cells)	days
scan_avg_datenum	datenum averaged over scan	days
sx	scan position, bad measurement points removed (nested cells)	m
sy	scan position, bad measurement points removed (nested cells)	m
sz	scan position, bad measurement points removed (nested cells)	m
sx_w_nan	scan position, bad measurement points replaced with NaNs (nested cells)	m
sy_w_nan	scan position, bad measurement points replaced with NaNs (nested cells)	m
sz_w_nan	scan position, bad measurement points replaced with NaNs (nested cells)	m
vlos	measured line-of-sight velocity (nested cells)	m/s
focal	lidar focal length (nested cells)	m
quality	metric related to quality of measurement (nested cells)	
power	metric for power of returned signal (nested cells)	
lidar_roll	lidar roll angle (right-hand rotation sx-axis) (nested cells)	rad
lidar_pitch	lidar pitch angle (right-hand rotation sy-axis) (nested cells)	rad
lidar_temp	lidar CRIO temperature (nested cells)	degC
scan_avg_turbinez01_yawHeading	turbine yaw heading averaged over scan	degN
scan_avg_metz01_wsSonic32m	32m sonic wind speed averaged over scan	m/s
scan_avg_metz01_wdSonic32m	32m sonic wind direction averaged over scan	degN
scan_wakePosition_lidarAxis	tracked wake center in lidar axis coordinates (nested cells)	<i>sx</i> (m), <i>sy</i> (m), <i>sz</i> (m)
scan_wakeBoundary_lidarAxis	tracked wake boundary in lidar axis coordinates (nested cells)	<i>sx</i> (m), <i>sy</i> (m), <i>sz</i> (m)
scan_avg_metz01_wdVane29m	vane wind direction averaged over scan	degN
lidPos	lidar position in lidar axis coordinates	<i>sx</i> (m), <i>sy</i> (m), <i>sz</i> (m)
variables	list of variable names and units	

### 3 National Instruments CompactRIO

The National Instruments CompactRIO (CRIO) provides the platform for turbine control and data acquisition at the SWiFT site. Data from the meteorological towers and turbines consists of both digital RS-422 serial communications and analog voltage signals and therefore different interface modules are connected to the CRIO. Digital signals are acquired by NI 9871 serial interface modules. Turbine analog signals are acquired by NI 9205, which have a  $-10 - 10$  V full-scale range with 16-bit resolution, while met tower analog signals are acquired by NI 9239, which have  $-10 - 10$  V full-scale range with 24-bit resolution. The SWiFT site time synchronization is provided by Global Positioning System (GPS) time stamps in the International Atomic Time (TAI) standard.

## 4 Meteorological Towers

### 4.1 Sonic Anemometers

Five SATI Series ‘A’ style probe ultrasonic anemometers from ATI Technologies Inc. are located at 10 m, 18 m, 32 m, 45 m, and 58 m above the ground on the METa1 and METb1 towers. The anemometers sample data at 100 Hz and measure  $u$ ,  $v$ , and  $w$  velocity components of the wind, as well as the temperature,  $T$ , based on the time of flight of a sound signal and the speed of sound calculation. In the provided data, the  $u$  vector points North,  $v$  points West, and  $w$  points up, as shown in Figure 2, which provides the SWiFT site coordinate system. The anemometers output data using the RS-422 serial protocol. Occasionally this signal has a spurious spike. The provided data are quality controlled to remove spikes using the median absolute deviation. The median window has a length 3,000 data points (30 seconds). Data more than four standard deviations away from the median are removed, and appear as NaN. Early sonic anemometer data sets (prior to January 20<sup>th</sup>, 2017) used time stamps supplied by the CRIO. Large time drifts on the order of minutes relative to the GPS synced data were observed with this method and corrected for using  $u$  and  $v$  velocity component data sampled at 20 Hz with GPS time stamps. Since January 20<sup>th</sup> 2017, all sonic anemometer data are sampled at 100 Hz with GPS time stamps. Thus, all of the Quality Assured and Quality Controlled (QA/QC) data provided has GPS-synced time stamps. In addition to the time stamp correction, the  $u$ ,  $v$ , and  $w$  velocity components have been transformed from their raw orientation to the  $u$ ,  $v$ , and  $w$  coordinate system of the SWiFT site. The roll and pitch rotation correction was determined by minimizing the standard deviation of the vertical velocity component as a function of wind direction for 60 minute averages over 1.5 months [2]. Data bins acquired with large wind direction changes or too high/low turbulence intensity were not included in the analysis. The yaw angle correction was calculated through comparisons with the calibrated wind vane and verified through total station theodolite (TST) measurements of the boom arms. Note that even though the sonic anemometers sample data at 100 Hz, frequencies above 20 Hz are likely contaminated by met tower dynamics.

### 4.2 Cup Anemometers

Three Wind Sensor First Class Advanced cup anemometers from Thies Clima are located 18 m, 31.5 m, and 45 m above the ground. The analog sensors output a frequency that is proportional to wind speed, 21.8 Hz/m/s. The cup anemometers are located approximately at the rotor bottom, hub, and rotor top heights. Data are sampled at 20 Hz. Occasionally this signal has a spurious spike. The provided data are quality controlled to remove spikes using the median absolute

deviation. The median window has a length 3,000 data points (30 seconds). Data more than four standard deviations away from the median are removed, and appear as NaN.

### 4.3 Wind Vane

One Thies Clima Wind Direction Sensor First Class measures wind direction at the hub height, 29.5 m. It outputs an analog voltage that is proportional to compass wind direction. Data are sampled at 20 Hz. The wind vane was calibrated to the SWiFT coordinate system by aligning the wind vane to two distant land marks with measured GPS positions. Note that presently there is a consistent, small nonlinearity when comparing the wind vane to the each of the sonic anemometer measured wind directions. This behavior was observed during the QA/QC process discussed in the sonic anemometer section. The nonlinearity was removed in calculating the sonic anemometer orientation by assuming a slope of one in the comparison and assuming the difference between a linear and the nonlinear calibration should average to zero. The nonlinear response has not yet been removed in the provided data, but a table-top calibration will be applied in the near future.

### 4.4 Barometric Pressure

Two Met One Instruments Inc. 092 Barometric Pressure sensors output a 0 – 5 V signal. The device was configured for high altitude application with a full-scale range of 800 – 1000 mbar. Pressures sensors are located at 2 m and 27.5 m above the ground. Data are sampled at 20 Hz.

### 4.5 Relative Humidity

Met One Instruments Inc. provides the 593 Relative Humidity sensors located at tower heights 2 m, 27.5 m, and 56.5 m. These analog instruments output a 0 – 1 V signal for a 0 – 100% humidity full-scale range. Data are sampled at 20 Hz. The Relative Humidity acquired at a height of 56.5 m has a large amount a noise, likely due to a grounding issue that has not yet been resolved.

### 4.6 Temperature

Met One Instruments Inc. provides the 9250 temperature sensors located at tower heights 2 m, 27.5 m, and 56.5 m. These analog instruments output a 0 – 1 V signal for a -30 °C – 50 °C full-scale range. Data are sampled at 20 Hz. The temperature acquired at a height of 56.5 m has a large amount a noise, likely due to a grounding issue that has not yet been resolved.

## 5 Turbine Sensors

### 5.1 Nacelle Wind Sensor

The FT702LT Version 22 wind sensor, made by FT Technologies Ltd, uses acoustic resonance to measure wind speed and wind direction. This sensor only measures a lateral velocity parallel to the ground and gives no vertical component of wind speed. Data are sampled at 50 Hz, but only updated at 1 measurement per second. The provided data are quality controlled to remove spikes using the median absolute deviation. The median window has a length 3,000 data points (30 seconds). Data more than four standard deviations away from the median are removed, and appear as NaN.

## 5.2 Yaw Heading

US Digital provides the HD25A absolute, optical, rotary encoder. The default 3600 counts/revolution is used to keep track of the nacelle yaw angle relative to the cardinal direction coordinate system. The encoder provides a resolution of 1 pulse per 0.01 degrees with an additional gear ratio providing a yaw heading resolution of 0.001 degrees. Data are sampled at 50 Hz. The absolute yaw position of the yaw encoder was calibrated using TST measurements of bolts along both sides of the nacelle bed plate. The bolt position measurements were least-squares fit with planes corresponding to the sides of the bed plate. The nacelle centerline was calculated as the average between the two planes. The nacelle centerline was transformed to the SWiFT coordinate system using site surveying markers that indicate true North. The TST calibration of the yaw encoder was verified with a plumb bob used to align the low-speed shaft with a surveying marker.

## 5.3 Azimuth Angle

The MIR 3000F HDmag Flex sensing head and magnetic belt, made by Gaumer Group, function as an incremental encoder with magnetic sensing. The magnetic belt is wrapped around the circumference of the low speed shaft, and the sensing head measures the rotational velocity of the shaft and the absolute azimuthal angle. Data are sampled at 50 Hz. The azimuth angle has not yet been calibrated to the zero angle position of the rotor.

## 5.4 Low Speed Shaft Tachometer

Carlo Gavazzi provides the DU10E inductive proximity sensor. The sensor provides a digital output by measuring the passing of 14 equally spaced flag-shaped sensor targets on the low-speed shaft. The angular velocity is calculated from the time between rising edges per 25.71 degrees. Data are sampled at 50 Hz.

## 5.5 High Speed Shaft Tachometer – Smoothed

Telemecanique provides the XS1M18PA370 inductive proximity sensor. The sensor measures 3 equally spaced lobes on the high speed shaft that pass the sensor providing a digital output. The angular velocity is calculated from the time per 360 degrees and updated at every 120 degrees. A moving average with a 24 ms window is used to smooth the measurement prior to logging the data at 50 Hz.

## 5.6 Generator Power and Generator Torque

Power and torque are reported by the ABB ACS800-17 Variable Frequency Drive. The power and torque values are updated with a resolution of 0.3 kW and 0.16 Nm, respectively, and the data are logged at 50 Hz. A 100 ms filter is applied to the generator torque data before logging

## 5.7 Blade Pitch

The blade pitch is controlled by the traverse tube extension through a pitch linkage. The kinematics have been modeled in detail and Figure 5 shows the relationship between the measured traverse tube extension in meters, and the blade pitch in degrees. A blade pitch of 1 degree is used during Region 2 and 2.5 of power generation, and the blade feathers towards 88 degrees in Region III and shutdown to shed load.

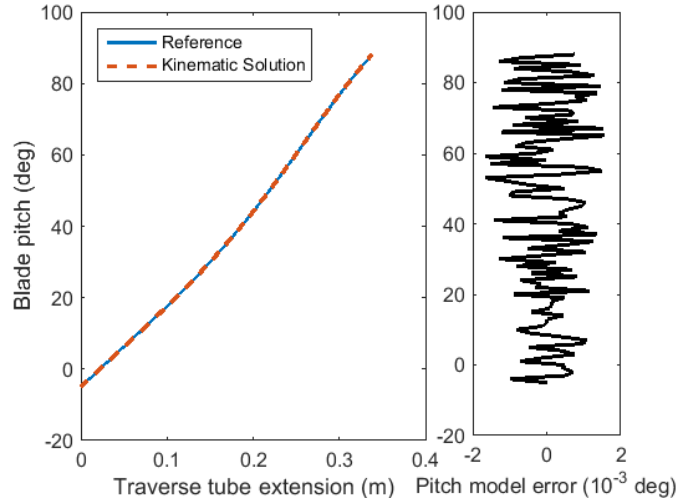


Figure 5. Relationship between the measured traverse tube extension (m) and blade pitch (deg).

## 6 Lidar Data

The wind turbine wake is characterized using the Technical University of Denmark (DTU) SpinnerLidar (Figure 6). Additional SpinnerLidar information can be found in Refs. [3-8]. The SpinnerLidar is a continuous-wave (CW) lidar that is currently configured to stream averaged Doppler spectra at a rate of 492 measurements per second. Typical data sets provide 2 s scans with 984 points per scan (Figure 7) prior to the removal of bad data points through the quality assurance and quality control (QA/QC) process. The SpinnerLidar has the ability to rapidly cycle through different focal lengths. Some data sets provide data with a constant focal length while others scan through multiple focal lengths. The lidar changes focal length in the same amount of time as a full scan and multiple scans are possible at a given focal length during the focal length cycle. Data points acquired while the lidar is changing focal length are removed in the QA/QC process.

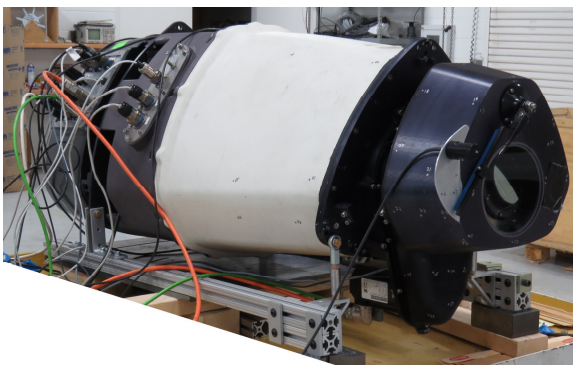


Figure 6. Images of the DTU SpinnerLidar.

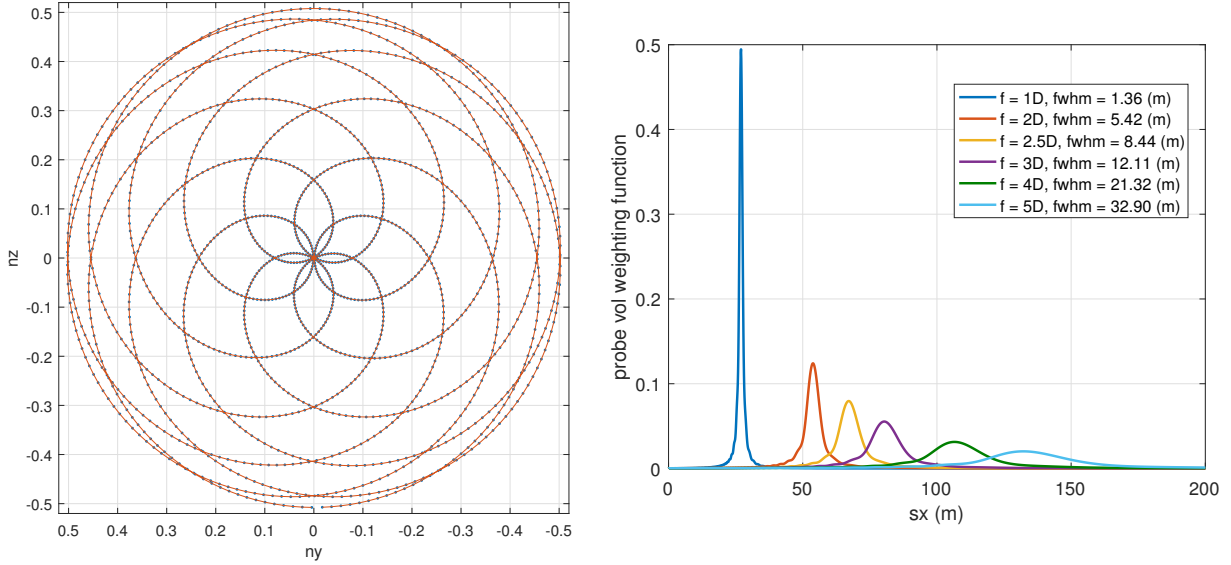


Figure 7. Calibrated DTU SpinnerLidar scan points in normalized lidar coordinates and lidar probe volume weighting function vs focal length.

The SpinnerLidar calculates the line-of-sight velocity from the returned Doppler spectra by calculating the centroid of frequencies observed within the probe volume above a noise threshold. Future documentation will outline the lidar QA/QC process in greater detail, but briefly, the method removes data points that have a low level of laser signal return relative to the noise threshold as well as points contaminated with laser signal returns from stationary objects. The removal of points with laser returns from stationary objects primarily removes points contaminated with ground returns and boresight returns. The boresight returns are due to laser reflections from the outer window and appear at the center of the scan pattern. Sometimes this removal includes points due to returns from the met towers and neighboring SWiFT wind turbines.

The lidar measurement location is aligned and calibrated using the method provided in Ref. [9]. The measurements are transformed into the coordinate system in Figure 2 (referred to as the lidar coordinate system), where the  $sx$  direction is aligned with the centerline of the nacelle axial direction,  $sz$  is vertical, and  $sy$  is oriented to create a right-handed coordinate system. The location of the measurements in the lidar coordinate system are scaled from an initial normalized frame (which was calibrated in Ref. [9]) using the average focal length over the scan. The actual focal length at each measurement point can fluctuate as high as  $\pm 2$  m. This fluctuation is relatively small when compared to the probe volume length of the lidar (Figure 7) [10, 11]. The orientation and position of the lidar relative to the ground and nacelle was determined using total station theodolite (TST) measurements [9]. The lidar roll and pitch angles (Figure 8) are measured by a calibrated 3-axis accelerometer [9], and applied to the data to create the lidar coordinate system ( $sx$ ,  $sy$ ,  $sz$ ).

The origin of the coordinate system is centered along the nacelle yaw rotation axis and located at the base of the turbine foundation. The vertical coordinate in the lidar coordinate frame matches the vertical coordinate of the SWiFT site coordinate frame, and the SWiFT site x-y plane matches the lidar  $sx$ - $sy$  plane. Thus, the only difference between the coordinate systems is due to the yaw



heading of the turbine. The lidar coordinate system can be transformed into the SWiFT site coordinate system by applying a rotation around the  $sz$  axis with a magnitude corresponding to the yaw heading. The lidar coordinate system is implemented as a balance between ease of data use and limited levels of initial processing for the data user. Users of the data should be able to easily transform the lidar coordinate system to the cardinal direction coordinate system or wind direction coordinate system as needed.

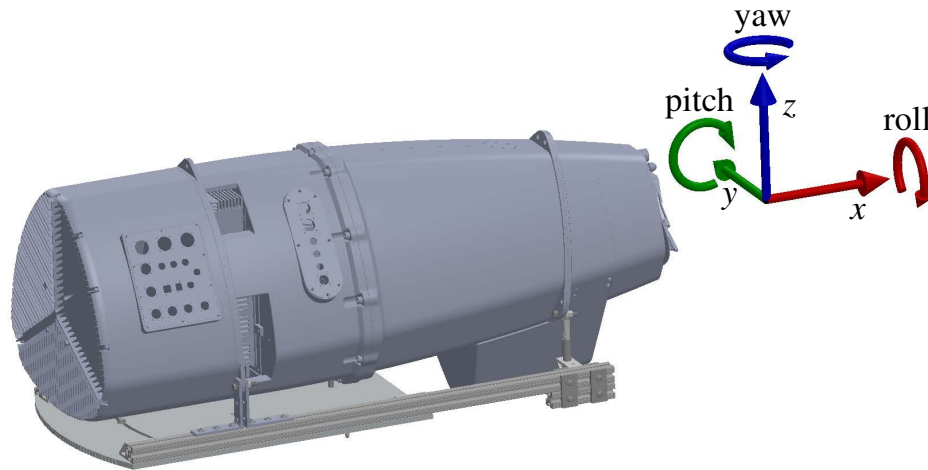


Figure 8. Lidar roll and pitch orientation schematic.

The time stamps on the lidar data are provided as datenum units. The SWiFT site natively acquires data using GPS synced TAI time stamps, while the lidar uses GPS synced Coordinated Universal Time (UTC) time stamps. The lidar time stamps have been adjusted to account for the 10 s base and leap seconds difference between the time standards and finally, to the supplied datenum units. Thus, the lidar data and SWiFT site data are highly synchronized.

The lidar data files are structured as variables with nested cell data types. Each file contains approximately 10 minutes of scans. The nested cell data types are needed because each scan can have a different number of points. Many of the provided lidar data channels are not required. The data has already been processed for QA/QC and the lidar coordinates have been transformed, so the quality, power, pitch, and roll channels are not necessary for the typical data user. The lidar data also contains a number of relevant met and turbine channels averaged over each scan. Figure 9 displays sample images from the lidar data at 1 – 5 D ( $D = 27\text{m}$ ) downstream of the turbine. The irregular scan pattern was interpolated to a regular grid using a smoothing surface fit, while the wake position was calculated using an image processing object detection method of the velocity wake deficit. The calculated wake center and boundary are provided in the data files but the regularized interpolated velocity points are not.

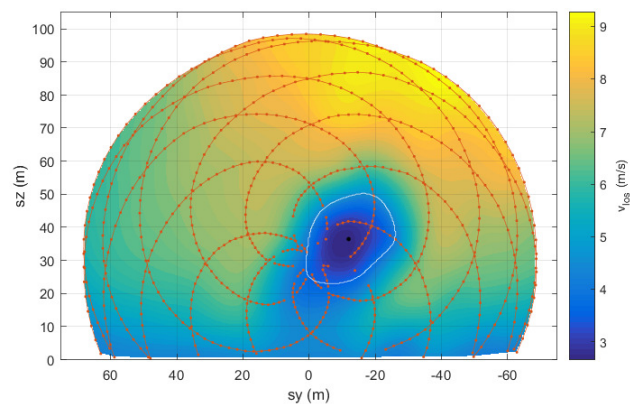
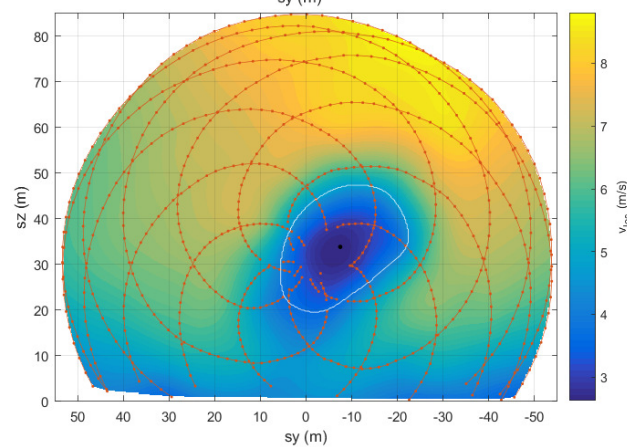
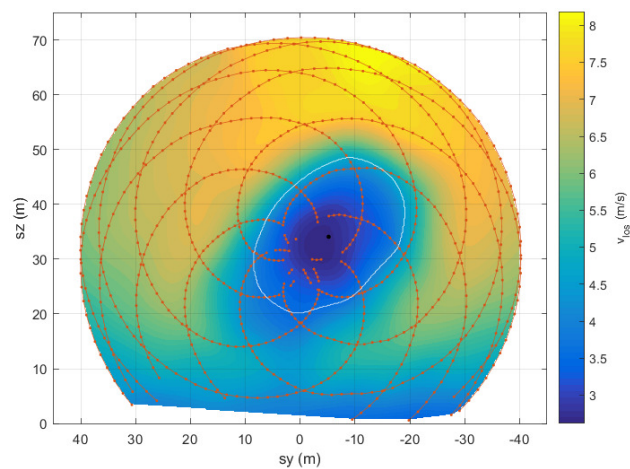
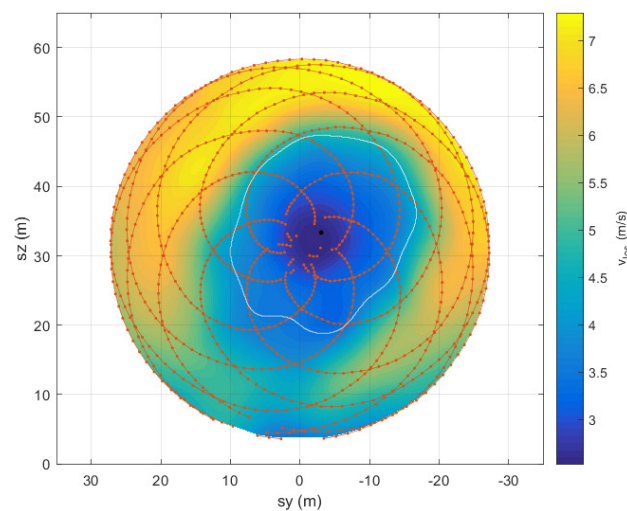
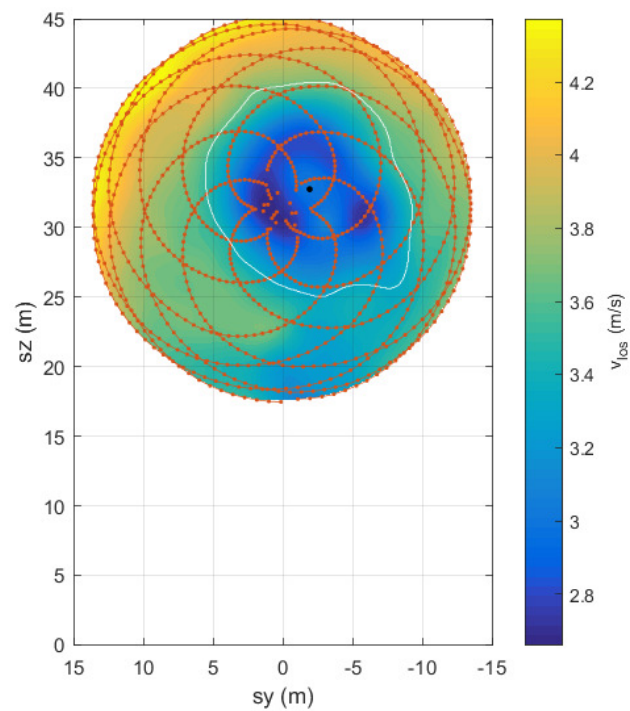
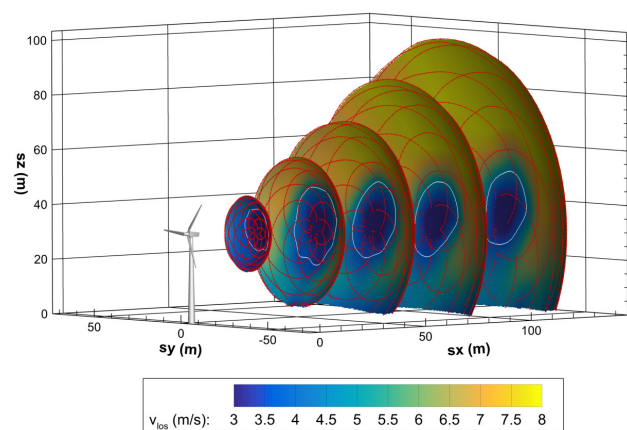


Figure 9. Example lidar measurements at 1 – 5 D.



## 7 References

1. Berg, J., Bryant, J., LeBlanc, B., Maniaci, D. C., Naughton, B., Paquette, J. A., Resor, B. R., White, J., and Kroeker, D. "Scaled Wind Farm Technology Facility Overview," *32nd ASME Wind Energy Symposium*. American Institute of Aeronautics and Astronautics, 2014.
2. Kelley, C. L., and Ennis, B. L. "SWiFT Site Atmospheric Characterization," *SAND-2016-2016*. Sandia National Laboratories, 2016.
3. Sjöholm, M., Pedersen, A. T., Angelou, N., Abari, F. F., Mikkelsen, T. K., Harris, M., Slinger, C., and Kapp, S. "Full two-dimensional rotor plane inflow measurements by a spinner-integrated wind lidar," *European Wind Energy Association Conference*. 2013.
4. Mikkelsen, T., Angelou, N., Hansen, K., Sjöholm, M., Harris, M., Slinger, C., Hadley, P., Scullion, R., Ellis, G., and Vives, G. "A spinner-integrated wind lidar for enhanced wind turbine control," *Wind Energy* Vol. 16, No. 4, 2013, pp. 625-643.  
doi: 10.1002/we.1564
5. Machefaux, E., Larsen, G. C., Troldborg, N., Hansen, K. S., Angelou, N., Mikkelsen, T., and Mann, J. "Investigation of wake interaction using full-scale lidar measurements and large eddy simulation," *Wind Energy* Vol. 19, No. 8, 2016, pp. 1535-1551.  
doi: 10.1002/we.1936
6. Angelou, N., and Sjöholm, M. "UniTTe WP3/MC1: Measuring the inflow towards a Nordtank 500kW turbine using three short-range WindScanners and one SpinnerLidar." DTU Wind Energy, 2015.
7. Churchfield, M., Wang, Q., Scholbrock, A., Herges, T., Mikkelsen, T., and Sjöholm, M. "Using High-Fidelity Computational Fluid Dynamics to Help Design a Wind Turbine Wake Measurement Experiment," *Journal of Physics: Conference Series* Vol. 753, No. 3, 2016, p. 032009.
8. Herges, T. G., Maniaci, D. C., Naughton, B. T., Mikkelsen, T., and Sjöholm, M. "High resolution wind turbine wake measurements with a scanning lidar," *EWEA Wake Conference, To Be Published*. 2017.
9. Herges, T. G., Maniaci, D. C., Naughton, B., Hansen, K., Sjöholm, M., Angelou, N., and Mikkelsen, T. "Scanning Lidar Spatial Calibration and Alignment Method for Wind Turbine Wake Characterization," *35th Wind Energy Symposium*. American Institute of Aeronautics and Astronautics, 2017.
10. Angelou, N., Mann, J., Sjöholm, M., and Courtney, M. "Direct measurement of the spectral transfer function of a laser based anemometer," *Review of Scientific Instruments* Vol. 83, No. 3, 2012, p. 033111.  
doi: 10.1063/1.3697728
11. Horváth, Z. L., and Bor, Z. "Focusing of truncated Gaussian beams," *Optics Communications* Vol. 222, No. 1-6, 2003, pp. 51-68.  
doi: [http://dx.doi.org/10.1016/S0030-4018\(03\)01562-1](http://dx.doi.org/10.1016/S0030-4018(03)01562-1)